Desalination and Water Treatment
www.deswater.com

doi: 10.5004/dwt.2020.25228

182 (2020) 208–219
April

Removal of copper and cadmium ions from contaminated groundwater by iron oxide/hydroxide-coated sand in the permeable reactive barrier technology

Mohammed B. Abdul-Kareem[a], Ayad A.H. Faisal[b,*]

[a]*Department of Environmental Engineering, College of Engineering, University of Baghdad, Baghdad, Iraq, email: Mohammed.bahjet73@gmail.com (M.B. Abdul-Kareem)*
[b]*Department of Environmental Engineering, College of Engineering, University of Baghdad, Baghdad, Iraq, Tel. +964 7904208688; email: ayadabedalhamzafaisal@yahoo.com (A.A.H. Faisal)*

Received 7 August 2019; Accepted 20 November 2019

ABSTRACT

Conversion of inert sand to the reactive material by plantation new active sites represented by iron oxide nanoparticles on its surface through simple impregnation can be considered the focal point of the present study. The conditions required to achieve the best impregnation were sand/ferric nitrate ratio of 2.5:1 g/g with initial pH of 11 which they specified based on the maximum values of cadmium sorption capacity (=0.8007 mg/g) and iron content (=1.1459 mg/g). The prepared coated sand by iron oxide (CSIO) has a good ability in the remediation of aqueous solution contaminated with copper and cadmium ions with removal efficiency exceeded the 92% under the best conditions of contact time, CSIO dosage, and initial pH equal to 1 h, 1 g/50 mL and 7 respectively. Pseudo-second-order and Langmuir models have described in a good manner the kinetic and isotherm sorption measurements with a coefficient of determination (≥0.9804) and the sum of squared errors (≤0.5496). Characterization tests for CSIO such as scanning electron microscopy, energy-dispersive X-ray spectroscopy, and X-ray diffraction proved that the iron oxide/hydroxide nanoparticles precipitated on the surface of sand particles and within the accessible pores. Fourier transform infrared spectroscopy analysis in combination with values of final pH revealed that the sorption mechanism was co-precipitation due to increase pH and complexation with surface of CSIO. Continuous tests proved that the longevity of the barrier in terms of breakthrough time was increased with a thicker bed in the permeable barrier technology and this barrier can be saturated with a contaminant as a function of the time. Also, results proved that the computer solution (COMSOL) Multiphysics has a good ability in the description of the transport of the contaminant in comparison with experimental measurements.

Keywords: Coated sand; Permeable barrier; Iron oxide; Isotherm; Kinetic

1. Introduction

The contamination with heavy metals in the surface and ground waters became a major environmental issue because these metals are non-biodegradable and tend to accumulate in living beings and to be the reason for different biological disorders. In spite of many metals are essential for constituents of the ecosystem at the trace level, their accumulation has a significant toxic impact. Moreover, there are a number of reactions that convert the heavy metals to compounds form within the bio-system and these compounds have carcinogenic effects even at very low concentrations [1,2]. Lead, copper, and cadmium often occur in the aquatic ecosystem. Copper is a trace element required for all living organisms which catalyzed the heme synthesis and iron absorption. Many problems for intestinal distress and

* Corresponding author.

stomach, kidney and liver damage, and anemia can result from the taken an excess quantity of copper [3]. In addition, cadmium can be caused many biological disorders in terms of nausea, diarrhea, muscle cramp and damage to bone marrow. Therefore, the United States Environmental Protection Agency (US EPA) specified the permissible limits for common heavy metals in the drinking water; for example, 1.3 mg/L for copper and 0.005 mg/L for cadmium [4].

Sorption, ion-exchange, coagulation/flocculation, precipitation, membrane filtration, and electrolysis are efficient methods used in the remediation of aqueous solutions polluted with heavy metals. The sorption method is based on the selection of the suitable materials that have a potential ability in the elimination of these contaminants. Low level of target metals, performance, cost-effectiveness, and selectivity are the most important points studied by previous literature [4,5].

Previous literature [6–14] were studied the possibility of using zero-valent iron, cement kiln dust, waste foundry sand, activated sludge, zeolite, composite cation exchanger and others in the treatment of aqueous solutions contaminated with heavy metals. Precipitates of iron oxides are considered efficient sorbents for inorganic and organic compounds [15–17]. Frequently, iron oxides exist as a fine powder and the difficulty of its separation from aqueous solution can be limited to the usage of this sorbent. The coating of iron oxide on solid supporting media was proposed and different media have been used. The natural sand was used primarily as a filter bed for filtration of raw water in the water supply systems; however, the removal capacity of sand material was found to be insignificant for heavy metal ions [18,19]. Due to its high permeability, modification of sand surface through the plantation of new active sites can be a good solution for producing medium that able to treat several types of heavy metals. In this direction, the impregnation of sand with manganese or iron could enable it to remove inorganic contaminants from aqueous solutions. The sand coated with iron oxide resulted from the fluidized and air aerated bed reactor was used for the treatment of aqueous solutions contaminated with arsenic ions [4]. Also, the natural iron oxide coated sand can be removed effectively the nickel and copper ions from aqueous solutions [20]. The simple sol–gel method had been used for coating the silica with iron and the efficiency of the prepared material was evaluated in the removal of cadmium ions. The sorption process was spontaneous and influenced by the pH of the water [21]. The utilization of manganese nitrate to obtain the manganese-impregnated natural sand was investigated in the previous studies and this can be achieved by adding the low dosage of manganese nitrate solution. Moreover, the particles of iron oxide can be aggregated onto the surface of different materials such as sand, silica, cement, activated carbon and sewage sludge [22–28]. The prepared materials were tested extensively for removing heavy metal cations including, Mn^{2+}, Cu^{2+}, Pb^{2+}, and Cd^{2+} or anion viz., Cr(VI). The present study investigated the ability of immobilized sand planted with the iron oxide nanoparticles to remediate aqueous solutions contaminated with copper and cadmium ions under different operational conditions. The possibility of using prepared material as a reactive bed in the permeable reactive barrier (PRB) technology for the treatment of contaminated groundwater can be the focal point that studied in the continuous tests and; however, required further investigation.

2. Materials and methods

2.1. Materials

Quartz sand was taken from the commercial market, washed with distilled water to remove any impurities and sieved before the use. This sand has an initial porosity of 0.45 with particle size distribution ranged from 0.6 to 1 mm and a specific gravity of 1.363. Copper and cadmium were selected as a representative of heavy metal contaminants. To simulate the water's copper and cadmium contamination, solutions of $Cu(NO_3)_2{\cdot}3H_2O$ and $Cd(NO_3)_2{\cdot}4H_2O$ (manufactured by HIMEDIA, India) were prepared with a concentration of 1,000 mg/L and these solutions were kept at room temperature. Every solution can be used as a stock solution to prepare any specific value of contaminant concentration and the pH of this solution was adjusted by adding 0.1 M HCl or 0.1 M NaOH as required.

2.2. Preparation of iron oxide/hydroxide-coated sand

A modified precipitation method was adopted to plant iron oxide nanoparticles on the surface of the sand as stationary phase [4]. This method is required to add a certain quantity (=1 g) of sand to 50 mL of an aqueous solution containing 2 g $Fe(NO_3)_3$. The pH of the mixture was adjusted to the desired value and this value can be ranged from 5 to 12. This mixture must be stirred for 3 h; then, dried at 105°C for 4 h and washed with de-ionized water to remove the unattached oxide until the pH of the washing water stabilized on a certain value within the range of (7–8). Thereafter, the solid particles should be dried at 105°C for 24 h and, finally, stored in a capped bottle for further use. The sand dosage and pH of aqueous solution are the major parameters used to evaluate the efficacy of the coating process based on the maximum adsorption capacity for the interaction of coated sand and water contaminated with cadmium as unique criteria in the evaluation under different preparation conditions. The characterization of coated sand was studied by the scanning electron microscopy (SEM) equipped with an energy-dispersive X-ray spectroscopy (EDS) (XFlash 5010; Bruker AXS Microanalysis, Berlin, Germany) operating in low-vacuum mode at 21°C and 55%–60% relative humidity; and the X-ray diffraction (XRD) data (Siemens X-ray diffractometer, D8 Advance, Bruker, Germany).

2.3. Batch experiments

Tests were implemented for determining the effect of contact time, initial pH, initial concentration and coated sand by iron oxide (CSIO) dosage on the performance of the sorption process. All Cu^{2+} and Cd^{2+} concentrations in the aqueous solution before and after interaction with CSIO can be measured by the atomic absorption spectrometer (AAS) (AA-7000 Shimadzu, Japan). Kinetic sorption tests were conducted over a contact time ranged from 0 to 180 min using 50 mL mixed with 0.5 g of CSIO in the conical flask for initial concentration of 10 mg/L Cu^{2+} and Cd^{2+} solution. The effect

of sorbent dosage on the sorption process was studied by changing its value from 0.03 to 1.5 g using 50 mL of aqueous solution in the 100 mL of flasks and the concentration of contaminant equal to 10 mg/L. In addition, the pH dependence data were obtained by taking a certain volume (=50 mL) with different concentrations (5–100) mg/L of Cu^{2+} and Cd^{2+} solutions where the values of pH in the range from 3 to 7 and CSIO quantity of 1 g. The flasks were kept stirred in an orbital shaker for 3 h at room temperature to complete the sorption process. At the end of each test, the samples were filtered by filter paper and the concentration of remaining metal in the aqueous solution can be measured by AAS. Further, the percentage of removal (R) of the metal ions can be determined by the following equation:

$$R = \frac{\left(C_0 - C_e\right)}{C_0} \times 100 \tag{1}$$

The sorption kinetic was fitted with the kinetic models namely; pseudo-first-order (Eq. (2)) and pseudo-second-order (Eq. (3)) as follows:

$$q_t = q_e\left(1 - e^{-k_1 t}\right) \tag{2}$$

$$q_t = \frac{t}{\left(\frac{1}{k_2 q_e^2} + \frac{t}{q_e}\right)} \tag{3}$$

where q_t and q_e (mg/g) are the sorbed amounts of contaminant onto the sorbent at time t and equilibrium respectively, k_1 is the pseudo-first-order rate constant (1/min), and k_2 is the pseudo-second-order rate constant (g/mg min). Then, the sorption data were fitted with Freundlich (Eq. (4)) and Langmuir (Eq. (5)) isotherm models illustrated below:

$$q_e = K_F C_e^{1/n} \tag{4}$$

$$q_e = \frac{q_{\max} b C_e}{1 + b C_e} \tag{5}$$

where C_e is the equilibrium concentration of metal ions in the bulk solution (mg/L), q_e is the number of metal ions sorbed onto the sorbent at equilibrium (mg/g). The K_F and n are the Freundlich constants which corresponded to the adsorption capacity (mg/g) and adsorption intensity respectively. Also, the b (L/mg) and $q_{\max}$ (mg/g) is the affinity constant and maximum adsorption capacity respectively.

2.4. Continuous experiments

The experimental setup (Fig. 1) used in the continuous tests was constructed of two perspex columns; each one has a height and diameter of 50 and 2.5 cm, respectively. The columns designated as column-1 and column-2 were supplied with three ports for taking the samples at the 10 cm (P1), 20 cm (P2), and 30 cm (P3) measured from the bottom. The ports were equipped with stainless steel fittings and

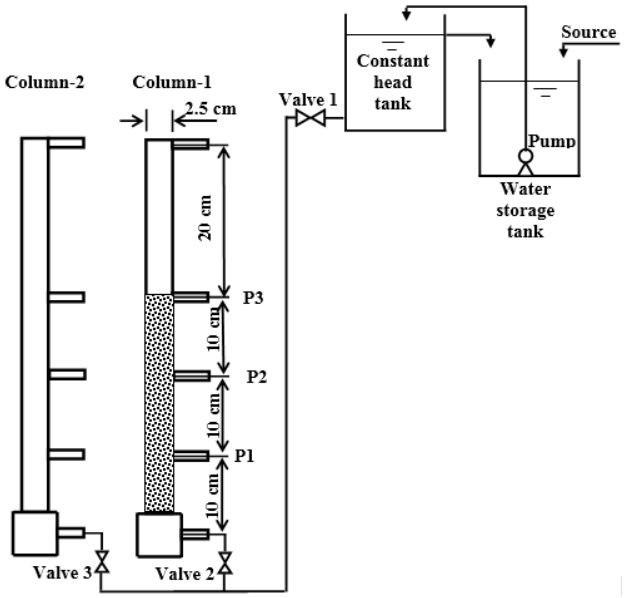

Fig. 1. Schematic diagram of the laboratory-scale column.

blocked with Viton stoppers. By using the syringe, water samples were taken from the centerline of the column at specified periods. The column-1 was packed with raw sand as reference bed and CSIO can be used to fill the column-2; then, distilled water can be injected from the bottom of the columns and forced upward through the medium. Thereafter, the water contaminated with copper and cadmium was introduced into the column based on the storage tank, flow-meter and two valves with an initial concentration of 20 mg/L. Monitoring of metal concentrations in the effluents from ports (P1 to P3) was conducted for a period of 13 d where samples can be withdrawn periodically and stored in the glass vails; then, they can be analyzed by AAS

3. Migration of dissolved contaminant

The multidimensional transport of the dissolved contaminant plume in the reactive and/or nonreactive medium is represented mathematically by the advection-dispersion equation. The mass balance equation applied to the control volume within the subsurface environment can be considered the cornerstone for the derivation of this equation. Hence, the general form of 1D advection-dispersion equation taking the sorption into account for the equilibrium case of solute transport in the saturated bed can be written as follows [29,30]:

$$D_z \frac{\partial^2 C}{\partial z^2} - V_z \frac{\partial C}{\partial z} = R \frac{\partial C}{\partial t} \tag{6}$$

where the first term in the left-hand side of this equation is the dispersion which means the transport of contaminant due to turbulent mixing, varied pathways, and concentration gradient, the second term in the same side is the advection that means the transport of contaminant with the flowing water, D_z is the dispersion coefficient (m^2/s) and resulted from summation of mechanical dispersion coefficient (D_{mech})

with molecular diffusion coefficient (D_0), V_z is Darcy velocity (m/s), C is the concentration of contaminant in the direction (z) after time (t).

The ability of sorbent bed to delay of contaminant transport can be expressed by the retardation factor (R). When the equilibrium sorption data are described by Langmuir model, this factor can be taken the following form [31]:

$$R = 1 + \frac{\rho b}{n}\left(\frac{q_{\max} b}{\left(1 + bC\right)^2}\right) \tag{7}$$

where n and r_b are the porosity and bulk density of the bed respectively.

To find the solution for Eq. (6), additional information about the physical state of the process is required. This information is supplied by boundary and initial conditions. Mathematically, the boundary conditions include the geometry of the boundary and the values of the dependent variable (i.e. concentration) or its derivative normal to the boundary [32]. In the present study, COMSOL Multiphysics version 3.5a (2008) was used to solve Eq. (6) numerically dependent on the finite element method. An early version of this program was called FEMLAB which established by graduate students to Germund Dahlquist based upon codes developed for a graduate course at the Royal Institute of Technology in Stockholm, Sweden (2005). This program runs the finite element analysis together with adaptive meshing and error control using a variety of numerical solvers.

4. Results and discussion

4.1. Coated sand by iron oxide

The pH of $Fe(NO_3)_2$ solution effect and the quantity of added sand have been evaluated based on the achieved maximum sorption capacity for removal of cadmium ions by CSIO as shown in Fig. 2. Cadmium was chosen to evaluate the coating process because of it more toxic from copper; however, it is expected that the copper has the same behavior of cadmium. The increase of the pH in the range from 5 to 12 for $Fe(NO_3)_2$ solution can be increased the sorption capacity of the coated sand. The increase in the capacity may be due to the modification of the sand surface as a result of coating with ferric hydroxide ($Fe(OH)_3$) precipitate [28]. This figure signified that there is a significant increase in the iron content precipitated on the sand surface which arrived at the maximum value of 1.201 mg/g at pH equal to 11 for a contact time of 3 h. When the surface of inert sand coated by iron oxide at pH of 11 for sand/ferric nitrate ratio of 0.1 g/g, the sorption capacity was increased to reach of 0.441 mg/g in comparison with sorption capacities corresponding to lower values of pH. Accordingly, the coating process can

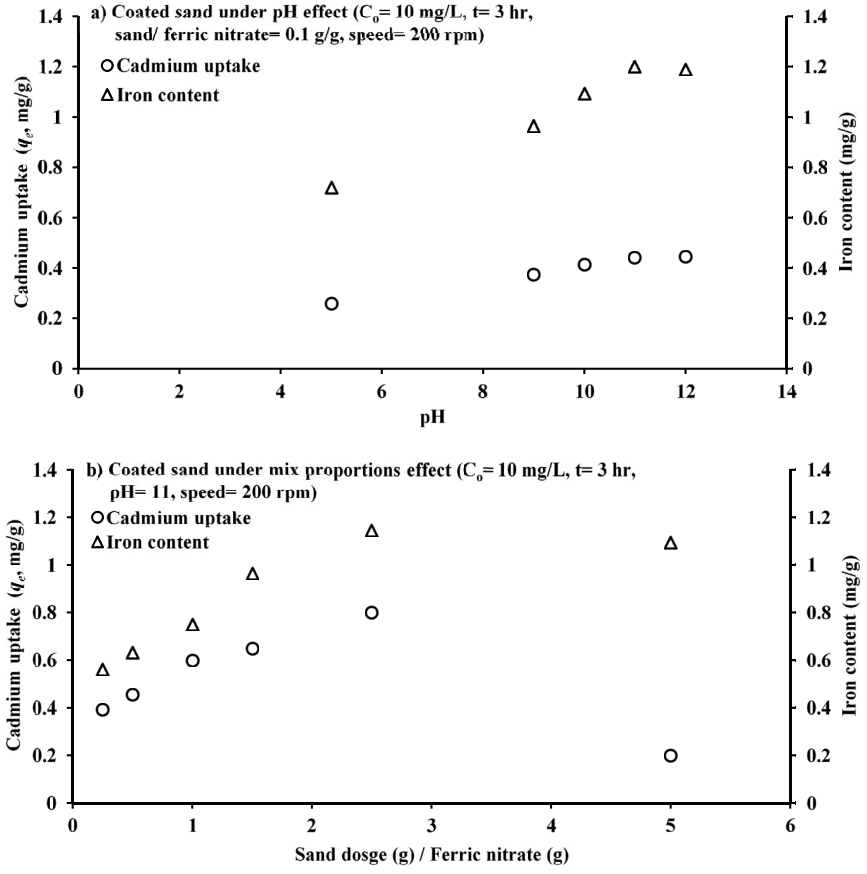

Fig. 2. Effect of (a) pH and (b) sand dosage on the efficacy of the coating process based on the cadmium sorption capacity onto CSIO.

be achieved at a pH equal to 11 because this value can be achieved the maximum values of sorption capacity and iron content.

Thereafter, the best quantity of used sand for coating can be specified by changing this quantity within the range from 0.5 to 10 g added to 50 ml solution mixed with 2 g of $Fe(NO_3)_2$. The sorption capacity of the coated sand for cadmium ions was increased as a result of the sand dosage increase from 0.5 to 5 g (0.25 to 2.5 sand dosage/ferric nitrate) as shown in Fig. 2b. When an excessive amount of sand was used (i.e. >5 g), the sorption capacity can be decreased because of the removal of uncoated iron oxide by washing at the end of the preparation process. Therefore, the sand dosage of 5 g (2.5 sand dosage/ferric nitrate) was chosen as the best value for the preparation of coated sand.

4.2. Equilibrium time

The equilibrium time should be determined to ensure the reaching for equilibrium concentrations. Fig. 3a shows the effect of contact time on the Cu^{2+} and Cd^{2+} removal using 0.5 g of CSIO added to 50 ml of contaminated solution for batch tests at room temperature. This figure demonstrates that the removal percentage of these contaminants significantly increased with an increase in the contact time with rapid rate at the initial times and this rate was slowed after approximately 15 min. The slower sorption may be due to the decrease in vacant sites on the surface of CSIO. The kinetic data showed that 1 h is sufficient to remove about 88% of metal ions under consideration and there is no significant change in the residual concentrations after this equilibrium time up to 3 h.

4.3. Dosage of CSIO

The quantity of CSIO has been changed with the range from 0.03 to 1.5 g for investigating the influence of CSIO dosage on the removal efficiency of Cu^{2+} and Cd^{2+} ions at room temperature as plotted in Fig. 3b. The batch experiments were implemented with a contact time of 1 h, initial pH of 5 and an agitation speed of 200 rpm. The increase of CSIO weight from 0.03 to 1 g can be caused by a significant improvement in the Cu^{2+} and Cd^{2+} removal percentage for an initial concentration of 10 mg/L. This is expected because the high amounts of CSIO will increase the vacant sites for collision with solute to enhance the removal of contaminants [33]. However, an increase in the quantity of sorbent beyond 1 g will not have a significant effect on the removal percentages because the quantities of Cu^{2+} and Cd^{2+} distributed between the aqueous solution and sorbent remain constant on the fixed value even with the further addition of dosage. The 1 g/50 mL was adopted as the best value of CSIO dosage and applied for remaining batch experiments.

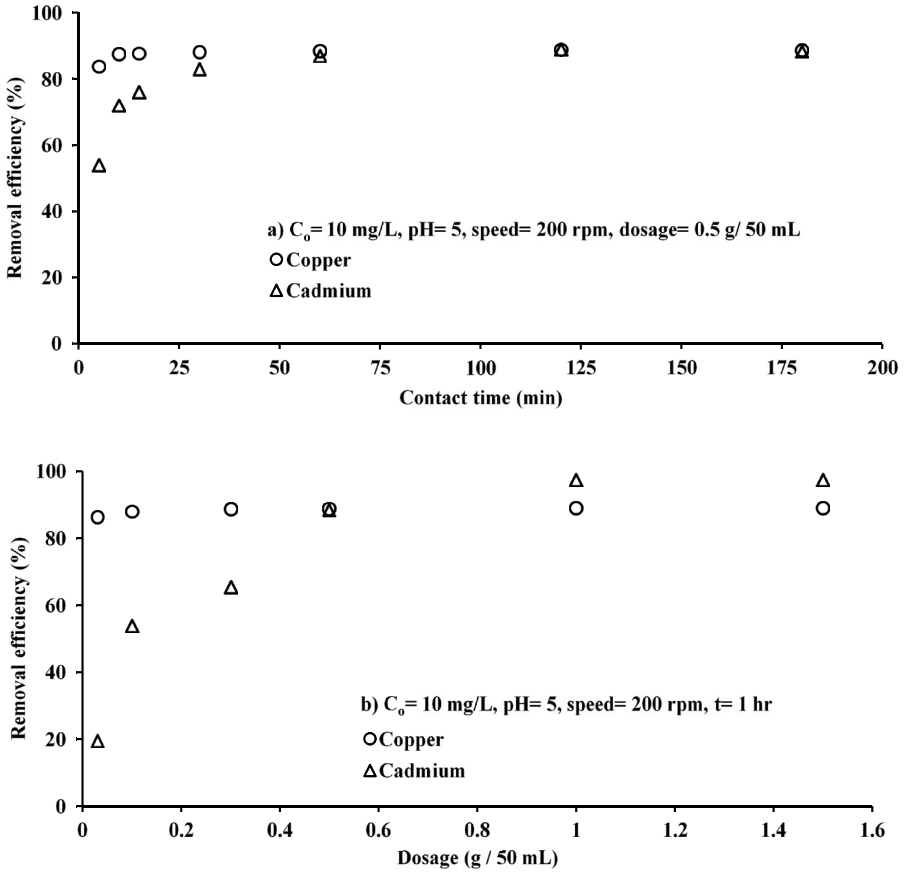

Fig. 3. Removal efficiency of Cu^{+2} and Cd^{+2} ions onto CSIO as a function of contact time and sorbent dosage.

4.4. Initial metal concentration and pH

The effect of initial concentration on the sorption efficiency of Cu^{2+} and Cd^{2+} ions was investigated within the range from 5 to 100 mg/L and adding the 1 g of sorbent into 50 mL of an aqueous solution. Fig. 4 revealed that the removal efficiencies of these metal ions by CSIO decreased from higher values (greater than 90%) to lower values due to an increase of initial concentration for a pH of 7. The presence of sufficient sites for sorbing of much more dissolved contaminants from aqueous solution may be the primary cause for this behavior. All metal ions available in the solution can able to interact with vacant binding sites at lower concentrations and, consequently, the uptake efficiency was high in comparison with higher concentrations. So, the treatment yield can be increased using the dilution of the water contaminated with high concentrations of heavy metal [34].

Fig. 4 also signified the effect of initial pH on the uptake of metal ions under consideration using CSIO and it seems that this uptake is greatly affected in response to the change of the solution pH. During the initial range of pH, the uptake of metal ions was increased gradually; quantitatively, increasing the pH from 3 to 7 can be caused a remarkable increase in the removal of Cu^{2+} and Cd^{2+} within the range of (53.7%–95.4%) for the initial metal concentration of 5 mg/L. The surface properties of CSIO and the nature of the metal ions present in the aqueous solution can be the key for an explanation of the pH dependence data for metals under consideration. The surface of sand mostly covered with nano-particles of iron oxide; hence, the properties of the bulk sand were greatly changed in the presence of impregnated iron oxide due to achieve the high values of removal percentages.

4.5. Sorption kinetic

"Solver" option in the Microsoft Excel 2016 for nonlinear regression was used to fit the measured kinetic data with the pseudo-first-order and pseudo-second-order kinetic models and the constants of the models are inserted in Table 1. It is clear from this table and Fig. 5 that the pseudo-second-order model has a high ability in the description of Cu^{2+} and Cd^{2+} sorption from aqueous solution onto CSIO because the coefficient of determination (R^2) greater than 0.9854 and sum of squared errors (SSE) not exceeded 0.001395. The concurrence with the pseudo-second-order model means that the predominant mechanism for the sorption process under consideration is the chemisorption.

4.6. Sorption isotherms

Freundlich and Langmuir's models are fitted with equilibrium sorption data for removal of copper and cadmium from the aqueous solution using CSIO where these

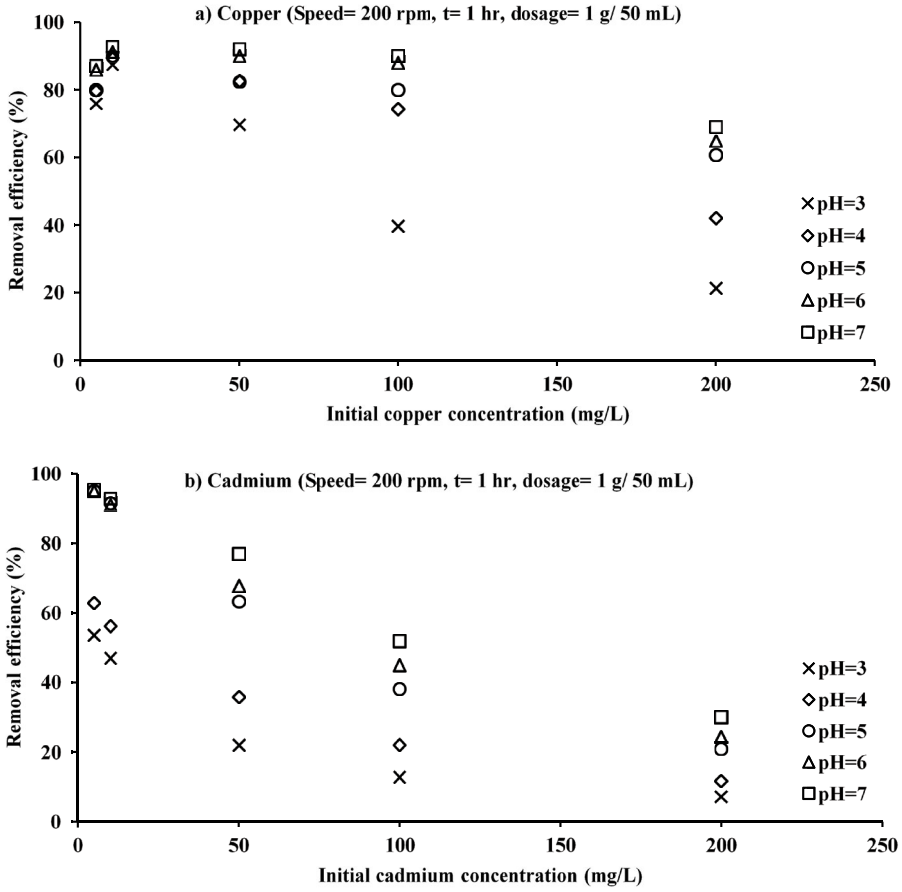

Fig. 4. Effect of initial concentration and pH on the uptake of Cu^{+2} and Cd^{+2} ions from aqueous solutions by CSIO.

models correlated between q_e and C_e [35]. The constants of the adopted models are determined by nonlinear regression [36] using the "Solver" option as listed in Table 2. This table certifies that the Langmuir model is the more suitable relationship for description of isotherm sorption data for different values of initial pH of the aqueous solution as clear from the magnitudes of R^2 (≥0.9804) and SSE (≤0.5496). However, the maximum sorption capacity was increased dramatically from 2.2366 at pH of 3 to reach 7.9957 at a pH of 7 for the uptake of copper ions onto CSIO and the same trend can be observed for cadmium ions with sorption capacity of 2.7661 mg/g at pH of 7. To evaluate the validity of the Langmuir model, the sorbed quantity was calculated using the equilibrium concentrations and isotherms parameters; then, compared with experimental measurements as shown in Fig. 6.

Table 1
Constants of the kinetic models for description of Cu^{+2} and Cd^{+2} ions sorption onto CSIO

Model	Parameter	Cu^{+2}	Cd^{+2}
Pseudo-first-order	q_e	0.87029	0.86466
	k_1	0.45451	0.18211
	R^2	0.9505	0.9547
	SSE	0.002383	0.004838
Pseudo-second-order	q_e	0.89188	0.91487
	k_2	1.57603	0.35329
	R^2	0.9854	0.9864
	SSE	0.000190	0.001395

4.7. Characterization of used materials

SEM micrographs of the used materials are presented the morphological characteristics for sand, CSIO, CSIO loaded with copper and CSIO loaded with cadmium as shown in Fig. 7. It is clear from Fig. 7a that the sand has

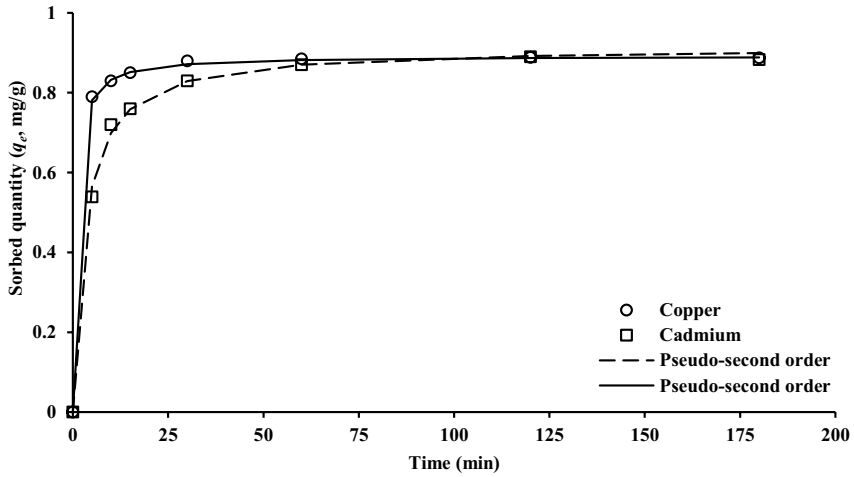

Fig. 5. Pseudo-second-order model for sorption of Cu^{+2} and Cd^{+2} ions onto CSIO in comparison with experimental measurements.

Table 2
Constants of sorption isotherm models used in the present study for uptake of Cu^{+2} and Cd^{+2} ions onto CSIO

Model		Parameter	pH				
			3	4	5	6	7
Cu^{+2}	Freundlich	K_F (mg/mg)(L/mg)$^{1/n}$	0.5770	0.8901	0.8536	1.1481	1.2683
		$1/n$	0.2799	0.3470	0.4634	0.4197	0.4214
		R^2, SSE	0.8936, 0.5503	0.8718, 1.8446	0.9278, 2.0936	0.9231, 2.4100	0.9272, 2.5457
	Langmuir	q_m (mg/g)	2.2366	4.7378	7.6425	7.5702	7.9957
		b (L/mg)	0.1714	0.0994	0.0559	0.0966	0.1112
		R^2, SSE	0.9843, 0.0591	0.9878, 0.1890	0.9804, 0.5496	0.9935, 0.2567	0.9952, 0.2340
Cd^{+2}	Freundlich	K_F (mg/mg)(L/mg)$^{1/n}$	0.1241	0.1634	0.5450	0.5558	0.6804
		$1/n$	0.3794	0.4502	0.3170	0.3588	0.3575
		R^2, SSE	0.9724, 0.0052	0.9678, 0.0217	0.9657, 0.0740	0.9797, 0.0622	0.9643, 0.1510
	Langmuir	q_{max} (mg/g)	0.7167	1.3240	1.9181	2.3424	2.7661
		b (L/mg)	0.0928	0.0646	0.3639	0.2190	0.2338
		R^2, SSE	0.9990, 0.0002	0.9995, 0.0004	0.9928, 0.0178	0.9903, 0.0416	0.9965, 0.0250

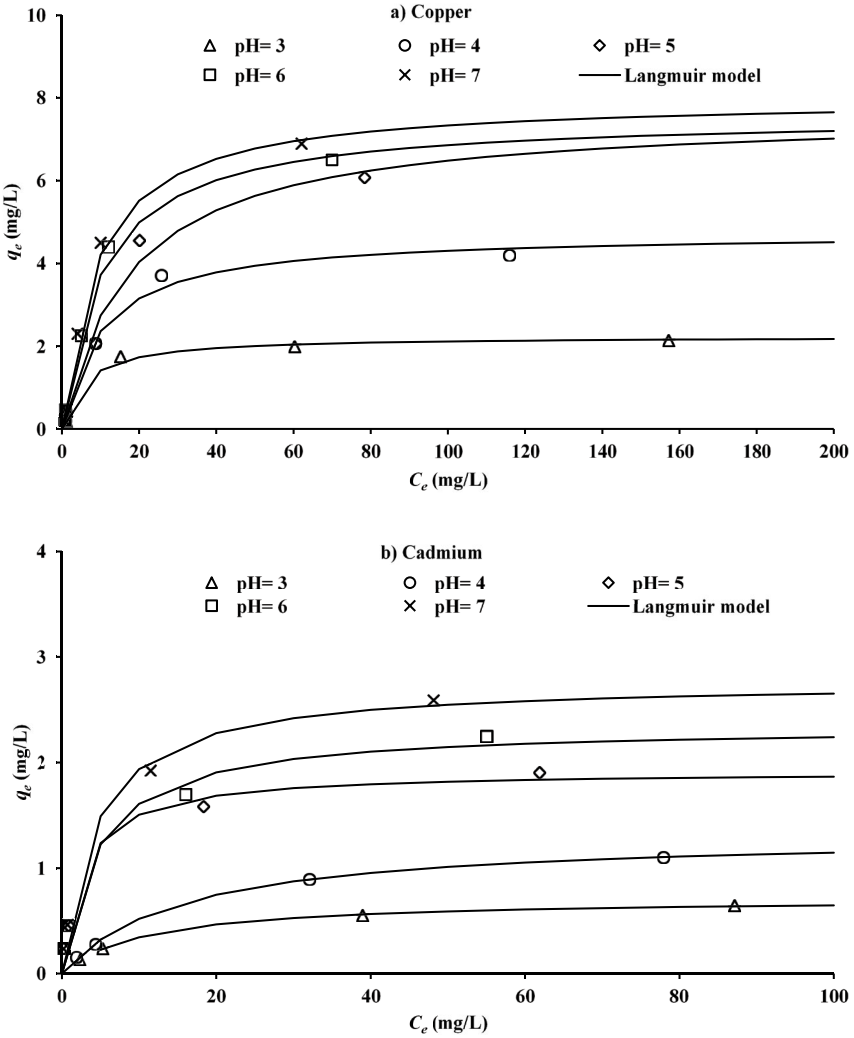

Fig. 6. Langmuir plot for sorption of (a) Cu^{+2} and (b) Cd^{+2} ions onto CSIO in comparison with experimental measurements.

heterogeneous, porous surface morphology with mean rod particles; however, its surface structure seems very compact and disordered. In spite of this sand don't have micro- or mesopores, surface roughness and cracks were visible. Fig. 7b elucidates that the iron oxide/hydroxide particles have a spherical morphology and they precipitated on the rod particles; also, intensive accumulation of nano-sized from these particles appears as a cluster. Moreover, the EDS data signified that the raw sand has a low content of iron (approximately 6.82%) and this percentage was reached 10.96% (by weight) after the coating process. The present results have been compatible with previous studies where the iron is mostly concentrated within the rough areas of the sand surface with non-uniform distribution of Fe and Si [4,24,37]. In addition, the present study certified that the iron oxide particles almost evenly distributed onto the sand surface. Fig. 7c explains the morphology and particle size of iron oxide loaded with copper and it is clear that the particles take the rose formation, while the cloud cadmium can be formed on the iron oxide particles loaded with cadmium as shown in Fig. 7d.

The sand before and after coating with iron oxide/hydroxide was investigated using XRD analysis and output data was plotted in Fig. 8a. It seems that there are distinct diffraction reflections occurred at values of 26.5, 27, 39.50, 47.39, 50.2, 54.6, 59.4, 64.99, and 67.67. The presence of silica in comparison with the standards mentioned by the Joint Committee on Powder Diffraction Standards (JCPDSs) may be the main cause of these reflections. The XRD analysis certified that the iron oxide was aggregated within the accessible pores and on the surface of the sand. Very low content of iron aggregated onto the surface of the sand will not cause the appearance of additional sharp reflections due to the coating process [24,38]. Previous studies were reported that the sand coated with an amorphous iron oxide had been converted to goethite and hematite at 150°C and hematite above 300°C [39].

The Fourier transform infrared spectroscopy (FTIR) analysis was achieved for CSIO before and after sorption for contaminants under consideration as shown in Fig. 8b to investigate the interaction between the contaminant and CSIO. The Fe–O (655 and 798 cm^{-1}) stretching band was

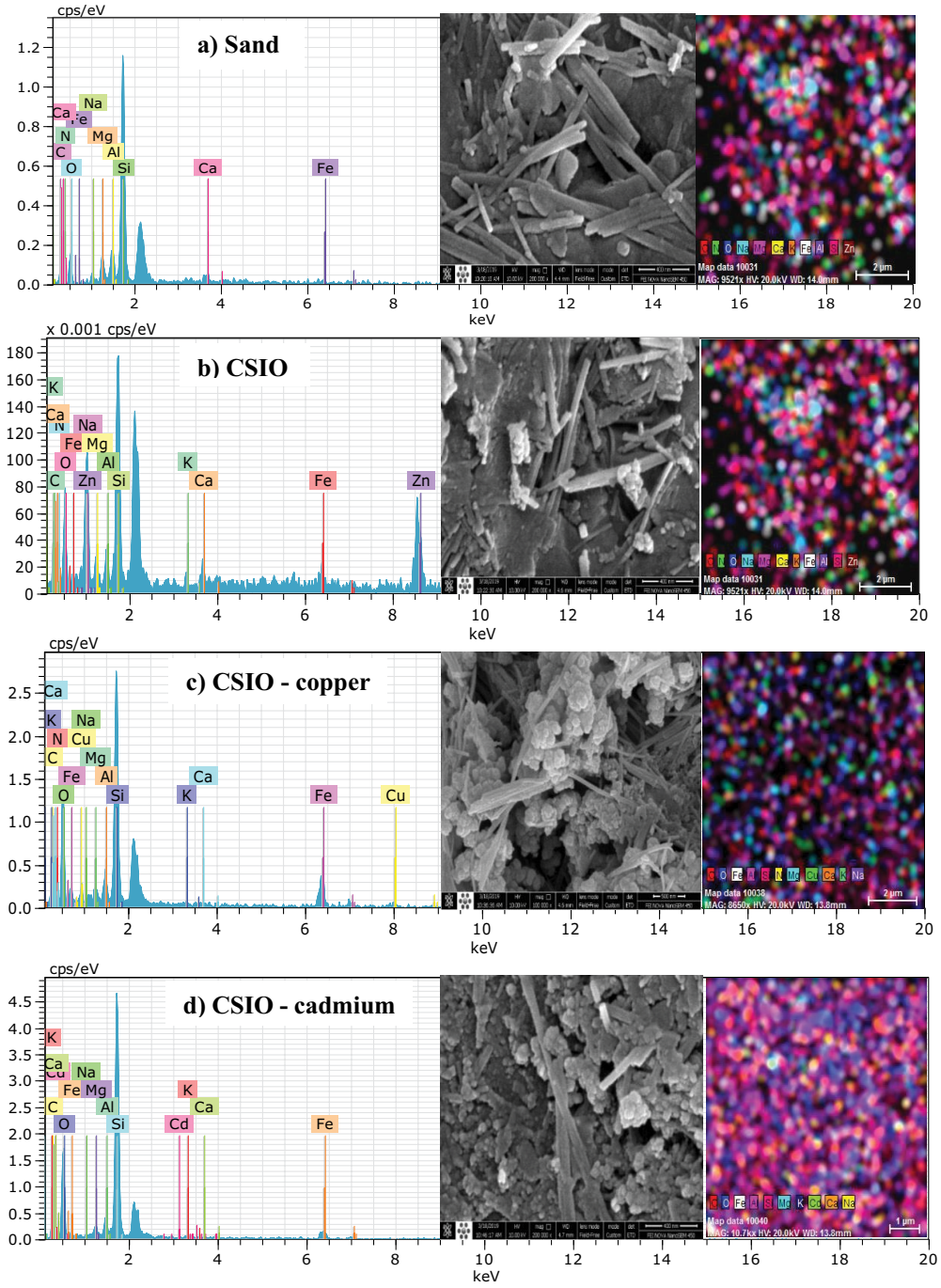

Fig. 7. SEM and EDS for (a) sand, (b) coated sand, (c) coated sand loaded with copper, and (d) coated sand loaded with cadmium.

found to shift when cadmium adsorption and there was no significant difference for copper adsorption. Therefore the interaction between cadmium and Fe–O can explain as in the following equation:

$$Fe-O+Cd^{2+}\leftrightarrow Fe-O\cdots Cd^{2+} \quad (8)$$

Raman spectra of Fe–OH (3,393 cm^{-1}) also suggested the formation of interaction between cadmium and copper which became more intense and can explain as follows:

For cadmium:

$$Fe-OH+Cd^{2+}\leftrightarrow Fe-OH\cdots Cd^{2+} \quad (9)$$

Or;

$$Fe-OH+Cd^{2+}\leftrightarrow Fe-O\cdots Cd^{2+}+H^{+1} \quad (10)$$

For copper:

$$Fe-OH+Cd^{2+}\leftrightarrow Fe-OH\cdots Cu^{2+} \quad (11)$$

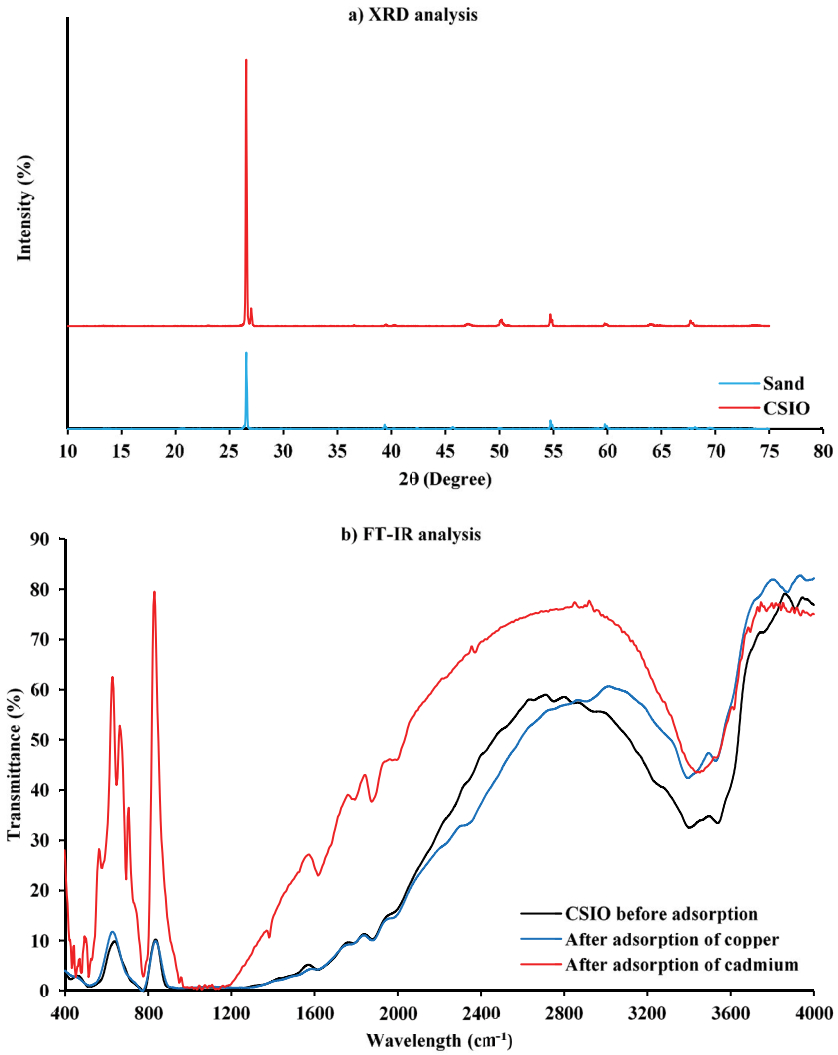

Fig. 8. (a) XRD pattern of sand before and after coating with iron oxide/hydroxide and (b) FTIR analysis for CSIO before and after the adsorption process.

Or;

$$Fe-OH+Cd^{2+}\leftrightarrow Fe-O\cdots Cu^{2+}+H^{+1} \quad (12)$$

There was no significant change in the silica group and this means that the sand is an inert material. On other hand, the measurement proved that the initial pH with values of 3, 4, 5, 6, and 7 were changed to become 7.5, 8.2, 8, 8.9, and 8.1 respectively at the end of the tests. This increase with pH was accompanied by the increase of the cadmium and copper ions removal; therefore, completive between H^+ and metal ions on surface made stronger ease for an increase of final pH. So, the adsorption mechanism was co-precipitation due to increasing pH and complexation with the surface of the adsorbent.

4.8. Breakthrough curves

The physical one-dimensional problem described previously for migration of contaminants in the CSIO bed was solved numerically by COMSOL Multiphysics 3.5a with the aid of the system properties, boundary conditions and initial condition illustrated in Table 3. Fig. 9 shows the

Table 3
Parameters and conditions used in the simulation of one-dimensional transport of copper and cadmium ions in the CSIO bed using COMSOL Multiphysics 3.5a

Item	Parameter	Value
PRB characteristics	Bed depth (cm)	30
	Porosity of CSIO	0.45
	Longitudinal dispersivity (α_L, cm)	6.49
	Bulk density (g/cm^3)	1.363
Initial condition	Initial concentration (mg/L)	zero
Boundary conditions	Concentration @ z = 0 (mg/L)	10
	Advective flux @ z = 30 cm	zero

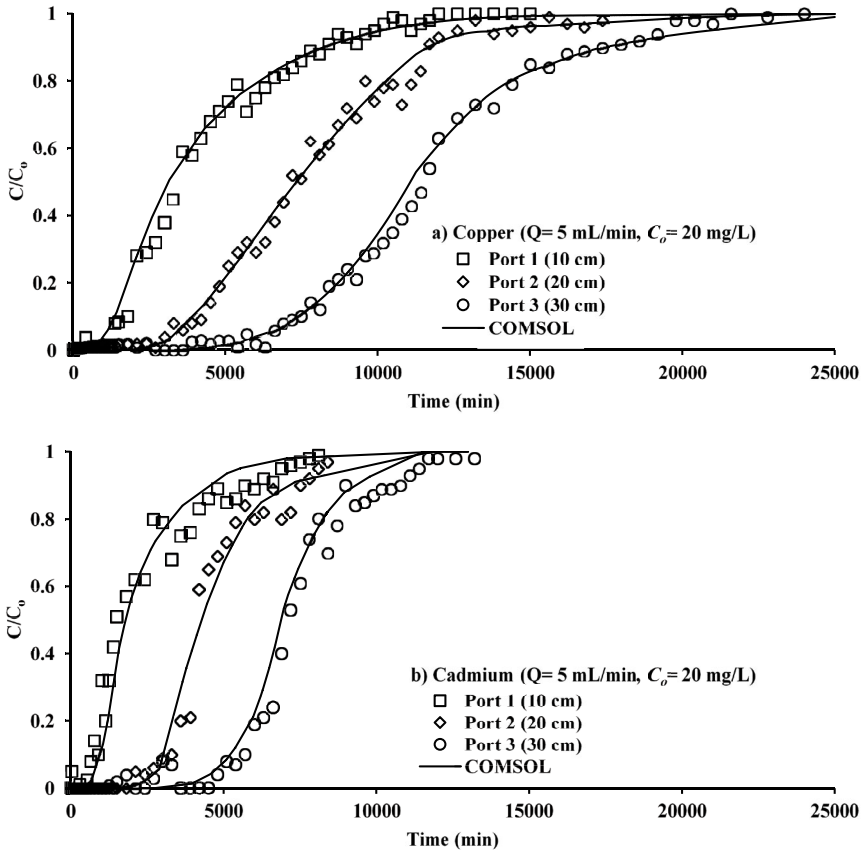

Fig. 9. Measured breakthrough curves for migration of (a) copper and (b) cadmium ions for different ports along the length of the column in comparison with predictions calculated by COMSOL Multiphysics 3.5a.

theoretical concentration lines of copper and cadmium ions calculated by the COMSOL software in comparison with measured values along the CSIO bed at a flow rate of 5 mL/min and initial concentration of 20 mg/L after many time intervals for column-2. The column-1 was always packed with raw sand as reference bed and the results proved that the effluent concentrations of metal ions under consideration in the port three (P3) not less than 9.5 mg/L for a duration not greater than 10 d. This means that the prepared CSIO had a significant role in the retardation of the propagation of the contaminant plume. The effect of bed thickness, varied from 10 to 30 cm, on metal treatment is illustrated in Fig. 9 and it can be seen that the thicker barrier has a good ability in the removal of metal ions in comparison with thinner beds. This is a logical behavior because the contact time between the aqueous solution and solid phase will increase and this causes a significant improvement in the treatment process. However, it seems that this barrier starts to saturate with metal ions due to increase in travel time and this causes a significant decrease in the retardation factor. Finally, a remarkable agreement between predicted and measured concentrations can be recognized (Fig. 9) with R^2 greater than 0.98.

5. Conclusions

The ordinary permeable nonreactive sand was converted into reactive material by planting nano-sized iron oxide/hydroxide particles on its surface using the impregnation process. This sand was named CSIO and tests proved its ability in the treatment of aqueous solutions contaminated with copper and cadmium ions. The best conditions for the coating process were achieved at the initial pH of the sand/ferric nitrate mixture of 11 and their weight ratio of 2.5 g/g. The results revealed that the values of contact time, CSIO dosage, and initial pH must be equal to 1 h, 1 g/ 50 mL and 7 respectively to achieve the removal efficiency not less than 92% for initial concentration of Cu^{2+} or Cd^{2+} ions of 10 mg/L. The pseudo-second-order model was able to describe the kinetic sorption data and this means that the chemisorption is the predominant mechanism in the removal process. Also, the Langmuir model was more suitable for the description of isotherm data with maximum sorption capacities arrived at 7.9957 and 2.7661 mg/g for copper and cadmium ions respectively onto CSIO. The characterization of sorbent material using SEM, EDS and XRD tests proved that the iron oxide/hydroxide nanoparticles have a spherical morphology and they precipitated on the surface of sand particles in the form of cluster; also, the iron oxide was aggregated within the accessible pores of the sand. Fixed bed column tests signified that the longevity of the CSIO was increased for thicker beds and the COMSOL numerical model can be described as the breakthrough curves in a good manner with a coefficient of determination not less than 0.98.

References

[1] P. Madoni, D. Davoli, G. Gorbi, L. Vescovi, Toxic effect of heavy metals on the activated sludge protozoan community, Water Res., 30 (1996) 135–141.

[2] A. Sigel, H. Sigel, R.K.O. Sigel, Metal Ions in Biological Systems, Volume 43 – Biogeochemical Cycles of Elements, Metal Ions in Biological Systems: Biogeochemical Cycles of Elements, CRC Press, 2005.

[3] J.L. Gardea-Torresdey, L. Tang, J.M. Salvador, Copper adsorption by esterified and unesterified fractions of *Sphagnum* peat moss and its different humic substances, J. Hazard. Mater., 48 (1996) 191–206.

[4] S. Lee, C. Laldawngliana, D. Tiwari, Iron oxide nano-particles-immobilized-sand material in the treatment of Cu(II), Cd(II) and Pb(II) contaminated waste waters, Chem. Eng. J., 195–196 (2012) 103–111.

[5] D. Sud, G. Mahajan, M. Kaur, Agricultural waste material as potential adsorbent for sequestering heavy metal ions from aqueous solutions – a review, Bioresour. Technol., 99 (2008) 6017–6027.

[6] H.M. Rashid, A.A.H. Faisal, Removal of dissolved trivalent chromium ions from contaminated wastewater using locally available raw scrap iron-aluminum waste, Al-Khwarizmi Eng. J., 15 (2019) 134–143.

[7] A.A.H. Faisal, T.R. Abbas, S.H. Jassam, Removal of zinc from contaminated groundwater by zero-valent iron permeable reactive barrier, Desal. Wat. Treat., 55 (2015) 1586–1597.

[8] A.A.H. Faisal, H.K. Jasim, Adsorption-precipitation mechanisms for cadmium removal from polluted water, Assoc. Arab Univ. J. Eng. Sci., 25 (2018) 110–125.

[9] A.A.H. Faisal, M.D. Ahmed, Remediation of groundwater contaminated with copper ions by waste foundry sand permeable barrier, J. Eng., 20 (2014) 62–77.

[10] A.H. Sulaymon, A.A.H. Faisal, Z.T. Abd Ali, Performance of granular dead anaerobic sludge as permeable reactive barrier for containment of lead from contaminated groundwater, Desal. Wat. Treat., 56 (2015) 327–337.

[11] A.A.H. Faisal, Z.A. Hmood, Groundwater protection from cadmium contamination by zeolite permeable reactive barrier, Desal. Wat. Treat., 53 (2015) 1377–1386.

[12] M. Naushad, Surfactant assisted nano-composite cation exchanger: development, characterization and applications for the removal of toxic Pb^{2+} from aqueous medium, Chem. Eng. J., 235 (2014) 100–108.

[13] M. Naushad, A. Mittal, M. Rathore, V. Gupta, Ion-exchange kinetic studies for Cd(II), Co(II), Cu(II), and Pb(II) metal ions over a composite cation exchanger, Desal. Wat. Treat., 54 (2015) 2883–2890.

[14] M. Naushad, T. Ahamad, B. Al-Maswari, A.A. Alqadami, S.M. Alshehri, Nickel ferrite bearing nitrogen-doped mesoporous carbon as efficient adsorbent for the removal of highly toxic metal ion from aqueous medium, Chem. Eng. J., 330 (2017) 1351–1360.

[15] K. Choo, S. Kang, Removal of residual organic matter from secondary effluent by iron oxides adsorption, Desalination, 154 (2003) 139–146.

[16] Y. Jeong, M. Fan, S. Singh, C. Chuang, B. Saha, J. Hans van Leeuwen, Evaluation of iron oxide and aluminum oxide as potential arsenic(V) adsorbents, Chem. Eng. Process., 46 (2007) 1030–1039.

[17] R.R. Sheha, E.A. El-Shazly, Kinetics and equilibrium modeling of Se(IV) removal from aqueous solutions using metal oxides, Chem. Eng. J., 160 (2010) 63–71.

[18] D. Tiwari, M.R. Yu, M.N. Kim, S.M. Lee, O.H. Kwon, K.M. Choi, G.J. Lim, Potential application of manganese coated sand in the removal of Mn(II) from aqueous solutions, Water Sci. Technol., 56 (2007) 153–160.

[19] S. Lee, W. Kim, C. Laldawngliana, D. Tiwari, Removal behavior of surface modified sand for Cd(II) and Cr(VI) from aqueous solutions, J. Chem. Eng. Data, 55 (2010) 3089–3094.

[20] N. Boujelben, J. Bouzid, Z. Elouear, Adsorption of nickel and copper onto natural iron oxide-coated sand from aqueous solutions: study in single and binary systems, J Hazard. Mater., 163 (2009) 376–382.

[21] M. Waseem, S. Mustafa, A. Naeem, G.J.M. Koper, K.H. Shah, Cd^{2+} sorption characteristics of iron coated silica, Desalination, 277 (2011) 221–226.

[22] M.M. Benjamin, R.S. Sletten, R.P. Bailey, T. Bennett, Sorption and filtration of metals using iron-oxide-coated sand, Water Res., 30 (1996) 2609–2620.

[23] C.H. Lai, S.L. Lo, H.L. Chiang, Adsorption/desorption properties of copper ions on the surface of iron-coated sand using BET and EDAX analyses, Chemosphere, 41 (2000) 1249–1255.

[24] Y. Xu, L. Axe, Synthesis and characterization of iron oxide-coated silica and its effect on metal adsorption, J. Colloid Interface Sci., 282 (2005) 11–19.

[25] S. Kundu, A.K. Gupta, Analysis and modeling of fixed bed column operations on As(V) removal by adsorption onto iron oxide-coated cement (IOCC), J. Colloid Interface Sci., 290 (2005) 52–60.

[26] R.L. Vaughan Jr., B.E. Reed, Modeling As(V) removal by a iron oxide impregnated activated carbon using the surface complexation approach, Water Res., 39 (2005) 1005–1014.

[27] N. Zhang, L.S. Lin, D. Gang, Adsorptive selenite removal from water using iron-coated GAC adsorbents, Water Res., 42 (2008) 3809–3816.

[28] T. Phuengprasop, J. Sittiwong, F. Unob, Removal of heavy metal ions by iron oxide coated sewage sludge, J. Hazard. Mater., 186 (2011) 502–507.

[29] C.W. Fetter, Contaminant Hydrogeology, 2nd ed., Prentice-Hall, New Jersey, ISBN: 0-13-751215-5, 1999.

[30] L. Elango, Numerical Simulation Groundwater Flow and Solute Transport, Allied Publishers Pvt. Ltd., 751, Anna Salai, Chennai-600 002, ISBN:81, 2005.

[31] A.A.H. Faisal, Effect of pH on the performance of olive pips reactive barrier through the migration of copper-contaminated groundwater, Desal. Wat. Treat., 57 (2016) 4935–4943.

[32] B. Barnett, L.R. Townley, V. Post, R.E. Evans, R.J. Hunt, L. Peeters, S. Richardson, A.D. Werner, A. Knapton, A. Mboronkay, Australian Groundwater Modeling Guidelines, Water Lines Report Series No. 82, June 2012.

[33] B.M.W.P.K. Amarasinghe, R.A. Williams, Tea waste as a low cost adsorbent for the removal of Cu and Pb from wastewater, Chem. Eng. J., 132 (2007) 299–309.

[34] K. Rao, M. Mohapatra, S. Anand, P. Venkateswarlu, Review on cadmium removal from aqueous solutions, Int. J. Eng. Sci. Technol., 2 (2011) 81–103.

[35] O. Hamdaoui, E. Naffrechoux, Modeling of adsorption isotherms of phenol and chlorophenols onto granular activated carbon. Part I. Two-parameter models and equations allowing determination of thermodynamic parameters, J. Hazard. Mater., 147 (2007) 1–2.

[36] A.M. Brown, A step-by-step guide to non-linear regression analysis of experimental data using a Microsoft Excel spreadsheet, Comput. Methods Programs Biomed., 65 (2001) 191–200.

[37] V.K. Gupta, V.K. Saini, N. Jain, Adsorption of As(III) from aqueous solutions by iron oxide-coated sand, J. Colloid Interface Sci., 288 (2005) 55–66.

[38] D. Tiwari, C. Laldanwngliana, C.H. Choi, S.M. Lee, Manganese-modified natural sand in the remediation of aquatic environment contaminated with heavy metal toxic ions, Chem. Eng. J., 171 (2011) 958–966.

[39] S.-L. Lo, H.-T. Jeng, C.-H. Lai, Characteristics and adsorption properties of iron-coated sand, Water Sci. Technol., 35 (1997) 63–70.